SCIENTIFIC REPORTS

OPEN

SUBJECT AREAS:
BATTERIES
MECHANICAL AND STRUCTURAL PROPERTIES AND DEVICES
ELECTRONIC DEVICES

Received
27 June 2013

Accepted
30 September 2013

Published
18 October 2013

Correspondence and requests for materials should be addressed to W.T.Z. (wtzheng@jlu.edu.cn)

Ultrahigh capacitive performance from both $Co(OH)_2$/graphene electrode and $K_3Fe(CN)_6$ electrolyte

Cuimei Zhao, Weitao Zheng, Xin Wang, Hengbin Zhang, Xiaoqiang Cui & Haoxiang Wang

Department of Materials Science, Key Laboratory of Mobile Materials, MOE, and State Key Laboratory of Superhard Materials, Jilin University, Changchun 130012, PR China.

Pseudocapacitance is commonly associated to the reversible redox reactions from electrode materials, but the enhancement in pseudocapacitance that only relies on electrode materials is limited. Here, we explore the possibility of enhancing pseudocapacitance through both $Co(OH)_2$/graphene nanosheets (GNS) electrode and $K_3Fe(CN)_6$ electrolyte. With a good conductivity and favoring electron transfer, GNS are hybridized with $Co(OH)_2$ to improve the pseudocapacitance of $Co(OH)_2$, including enhancing its rate capability and electrochemical stability. Adding $K_3Fe(CN)_6$ into KOH electrolyte further enhances the pseudocapacitance via both directly contributing pseudocapacitance to $Co(OH)_2$/GNS and promoting the electron gain and loss of Co ions. This novel $Co(OH)_2$/GNS-$K_3Fe(CN)_6$/KOH electrode system shows an ultrahigh specific capacitance of 7514 Fg^{-1} at 16 Ag^{-1} in mixed 1 M KOH and 0.08 M $K_3Fe(CN)_6$, more than 100% coulombic efficiency, and long-term cycling stability (the capacitance retention is 75% after 20000 continuous charge-discharge cycles in mixed 1 M KOH and 0.04 M $K_3Fe(CN)_6$).

As the depletion of fossil fuels and environmental pollution leads to the accelerated development of renewable and clean energy conversion/storage systems, two types of electrochemical devices such as batteries and electrochemical capacitors (ECs) have been paid more attention. Batteries with high energy densities suffer from slow power delivery, whereas ECs exhibit high power but low energy densities. Hence both high energy and high power without sacrificing cycle life will be demanded for future electrochemical energy storage applications. This demand can be met by the ECs if their energy densities can be enhanced efficiently[1–7]. High power density, long cycle life and environment-friendly, compared to traditional batteries, make ECs promising energy storage devices in a wide range of applications, such as hybrid electric vehicles, mobile electronic devices, large industrial equipments and space or military devices, wherein relatively light weight and small size are desirable. However, the disadvantage of ECs including low energy densities has been identified as a major challenge for the capacitive storage science[2,4,8].

Electrochemical performance of the ECs depends on both electrode and electrolyte. For electric double layer capacitors (EDLCs) employed high-surface-area carbon materials as the electrode in aqueous or organic electrolytes[9–11], electric charges physically stored on the carbon particles in porous electrode layers are unfortunately limited, resulting in a low specific capacitance, around 150 Fg^{-1}[12,13]. Compared to carbon-based materials used in EDLCs, low-cost pseudo-capacitive active materials such as $Ni(OH)_2$, NiO, $Co(OH)_2$, Co_3O_4, MnO_2 et al. have much higher theoretical capacitance (above 1000 Fg^{-1}) because of the presence of faradaic redox reactions in aqueous electrolytes. However, faradaic redox reactions also exhibit a low rate capability and low cycling stability due to the poor conductivity[4,14,15]. With nanostructured carbon used as support for direct growth of active materials, nanostructured three-dimensional electrode architectures have been realized to tailor ionic and electronic transport and increase efficient utilization of pseudo-capacitive materials[16–19]. Although the combination of EDLC with pseudocapacitor electrode is able to improve the electrochemical performance of ECs effectively, the energy density cannot be improved significantly via only relying on the active electrode materials.

Very recently, there have been a few reports that redox additives are introduced into the electrolyte for carbon EDLCs to substantially enhance the capacitance via redox reactions of the additives between the electrode and electrolyte. For example, Wu et al[20]. have introduced phenylenediamine as a redox mediator into KOH electrolyte for the carbon-based supercapacitor, and a much higher specific capacitance (605.2 Fg^{-1}) than that (144.0 Fg^{-1}) with conventional KOH electrolyte has been achieved. Roldan et al[21]. have reported that via adding

electrochemically active compound quinone/hydroquinone (Q/HQ) into the H_2SO_4 electrolyte, an ultrahigh specific capacitance of 5017 Fg^{-1} has been obtained for carbon-based supercapacitor. The significantly improved capacitance, upon introduction of HQ into the electrolyte, attributes to that the faradaic reactions of the Q/HQ couples ($HQ \overset{2H^+ 2e^-}{\longleftrightarrow} Q$) contribute pseudocapacitance to the electrode. However, the working condition for realizing the reactions of these quinoid compounds is that $[H^+] > [Q]$ in electrolyte as unbuffered media. This working condition is not easily maintained, leading to a poor electrochemical stability. Alshareef et al[22]. have added the Q/HQ into H_2SO_4 electrolyte and found that the specific capacitance of rGO/PAni is enhanced. However, the specific capacitance of rGO/PAni-Q/HQ decreases to 64% of initial value after 50000 cycling at a relatively small current density 10 Ag^{-1}, which is close to that of rGO/PAni, meaning that the capacitance from Q/HQ disappears gradually. This demonstrates that the capacitance contributed by Q/HQ is not constant and stable. Senthilkumar et al[23]. have improved the capacitance for activated carbon materials through adding either KI or KBr into 1 M H_2SO_4 or Na_2SO_4 electrolyte. However, there is also a problem with the electrochemical stability for only relying on the pseudo-capacitive contribution from additive for EDLCs.

As for the pseudocapacitors, is it possible to improve the pseudocapacitance via introducing redox additives into electrolyte? So far, there have been few reports on this investigation except that Su et al[24]. have improved the capacitance of Co–Al layered double hydroxide (LDH) electrode through the addition of either $K_3Fe(CN)_6$ or $K_4Fe(CN)_6$ into KOH solution. The Co–Al LDH in mixed either $KOH/K_3Fe(CN)_6$ or $KOH/K_4Fe(CN)_6$ electrolytes exhibits an increased capacitance up to 712 and 317 Fg^{-1} at a current density of 2 Ag^{-1}, respectively, which is higher than that only in KOH solution (226 Fg^{-1}). This enhancement in capacitance can be ascribed to that $Fe(CN)_6^{4-}/Fe(CN)_6^{3-}$ promotes the electron gain and loss of Co ions during charging/discharging. However, no redox peaks from $Fe(CN)_6^{4-}/Fe(CN)_6^{3-}$ are observed. Also, unfortunately, the electrochemical stability for Co-Al LDH after introducing either $K_3Fe(CN)_6$ or $K_4Fe(CN)_6$ into electrolyte is not discussed, although there is a problem with the electrochemical stability for Co-Al LDH too.

As mentioned above, although more attention has been paid to investigating either electrode or electrolyte for enhancing the capacitance, no any efforts have been done to improve both the solid electrode and liquid electrolyte simultaneously for pseudocapacitors. In previous work, our obtained binder-free $Co(OH)_2$/GNS/Ni foam electrode exhibits a high rate capability and long-term cycle life, in which GNS provides a high electrical conductivity and high specific surface area, allowing rapid and effective charge transfer and electron transport. Hence GNS play an important role in improving the pseudocapacitance of $Co(OH)_2$, including enhancing its rate capability and electrochemical stability[25]. In this work, we aim at further improving the pseudo-capacitive behavior for $Co(OH)_2$/GNS electrode through adding $K_3Fe(CN)_6$ into KOH electrolyte, based on that $Fe(CN)_6^{3-}/Fe(CN)_6^{4-}$ redox pair has a high solubility and electrochemical activity. Our findings are that $Fe(CN)_6^{3-}/Fe(CN)_6^{4-}$ not only promotes electron gain and loss of Co ions, but also directly gives a contribution to the pseudocapacitance for $Co(OH)_2$/GNS-$KOH/K_3Fe(CN)_6$. Our designed and prepared $Co(OH)_2$/GNS-$KOH/K_3Fe(CN)_6$ shows an unusually high specific capacitance (7514 Fg^{-1} at 16 Ag^{-1} in mixed 1 M KOH and 0.08 M $K_3Fe(CN)_6$), more than 100% coulombic efficiency, and long-term cycling stability (the capacitance retention is 75% after 20000 continuous charge-discharge cycles in mixed 1 M KOH and 0.04 M $K_3Fe(CN)_6$).

Results

The XRD measurements for $Co(OH)_2$/GNS before electrochemical test and after 2000 charge-discharge cycles, in the mixed 1 M KOH and 0.04 M $K_3Fe(CN)_6$ solution, at the current density of 80 Ag^{-1}, show that XRD patterns of $Co(OH)_2$/GNS before electrochemical test and after 2000 cycles are almost the same, and no new diffraction peaks are detected after 2000 cycles (Supporting material 1). Also, the morphologies for original $Co(OH)_2$/GNS and $Co(OH)_2$/GNS after 2000 cycles are nearly the same (supporting material 2). XRD and SEM measurements confirm that the novel electrode-electrolyte system is stable.

In order to compare the redox reactions for $Co(OH)_2$/GNS before and after adding $K_3Fe(CN)_6$ into KOH electrolyte, the cyclic voltammograms (CV) measurements have been performed. Figure 1(a)–(c) display for three systems: (1) $Co(OH)_2$/GNS electrode in 1 M KOH aqueous solution ($Co(OH)_2$/GNS-KOH); (2) platinum plate electrode in mixed 1 M KOH and 0.04 M $K_3Fe(CN)_6$ aqueous solution (Pt-$KOH/K_3Fe(CN)_6$); (3) $Co(OH)_2$/GNS electrode in mixed 1 M KOH and 0.04 M $K_3Fe(CN)_6$ aqueous solution ($Co(OH)_2$/GNS-$KOH/K_3Fe(CN)_6$), at different scan rates (2, 5, 10, 25 and 50 mVs^{-1}) in the potential range of −0.2–0.5 V, respectively. Here, system 1 and 2 is chosen for comparison. For $Co(OH)_2$ active material as electrode, the oxidation and reduction reactions observe the following faradaic reactions:

$$Co(OH)_2 + OH^- \leftrightarrow CoOOH + H_2O + e^- \quad (1)$$

For system 1 with $Co(OH)_2$/GNS as electrode in 1 M KOH aqueous solution, as shown in Fig. 1(a), a reversible charge-transfer process is observed: the charging process corresponds to the oxidation of $Co(OH)_2$ to CoOOH, while the discharging process corresponds to the reduction of CoOOH to $Co(OH)_2$. The oxidation and reduction peaks appear at 0.033 V and 0.022 V, respectively, and the peak potential separation (ΔE_P) is 0.011 V at a scan rate of 2 mVs^{-1}. The oxidation peak upshifts and the reduction peak downshifts slightly with increasing scan rate. In addition, the peak current of anodic oxidation almost equals to that of the cathodic reduction for each curve. Hence the $Co(OH)_2$/GNS electrode exhibits a high electrochemical activity and good charge/discharge reversibility. This capacitance behavior can be explained by that GNS provides a high electrical conductivity and high specific surface area, allowing rapid and effective electron and ion transport, while $Co(OH)_2$ nanosheets grown on GNS realizes a fast charge transfer, providing a high electrochemical activity and redox reversibility. For system 2 with the platinum plate as electrode in mixed 1 M KOH and 0.04 M $K_3Fe(CN)_6$ aqueous solution, as shown in Fig. 1(b), a pair of reversible redox peaks are observed, where the oxidation peak is related to the charging process of $K_4Fe(CN)_6$ to $K_3Fe(CN)_6$ and reduced peak is from the reverse process, corresponding to the following reactions:

$$K_4Fe(CN)_6 \leftrightarrow K_3Fe(CN)_6 + e^- \quad (2)$$

The characteristic CV shape of $K_3Fe(CN)_6$ is not significantly influenced as the scan rate is increased. The redox reaction on platinum electrode is a fast and reversible electrochemical process, indicating that $K_3Fe(CN)_6$ has a high electrochemical activity. For system 3 with the $Co(OH)_2$/GNS as electrode in mixed 1 M KOH and 0.04 M $K_3Fe(CN)_6$ aqueous solution, as shown in Fig. 1(c), two symmetric anodic/cathodic pairs superimposed on a broad redox background are recognized, indicating that reversible redox reactions of $Co(OH)_2$ solid electrode and $K_3Fe(CN)_6$ liquid electrolyte occur simultaneously and independently, according to the equations (1) and (2).

The $K_3Fe(CN)_6$-dependent capacitive properties can be determined from the charge-discharge potential vs. time curve. Figure 2(a) and 2(b) show the charge-discharge potential vs. time curve for system 1 or 3 at high current density of 16 or 32 Ag^{-1} in the potential range of −0.1–0.45 V. From Fig. 2(a), the potential plateaus at about 0.05 V in charging process and 0.00 V in discharging processes correspond to the oxidation of $Co(OH)_2$ and the reduction of CoOOH, respectively. From Fig. 2(b), besides the potential plateaus at about 0.025 V in charging process and −0.025 V in discharging processes, corresponding to the redox reaction of $Co(OH)_2$, there are other potential plateaus at about 0.25 V in charging process and

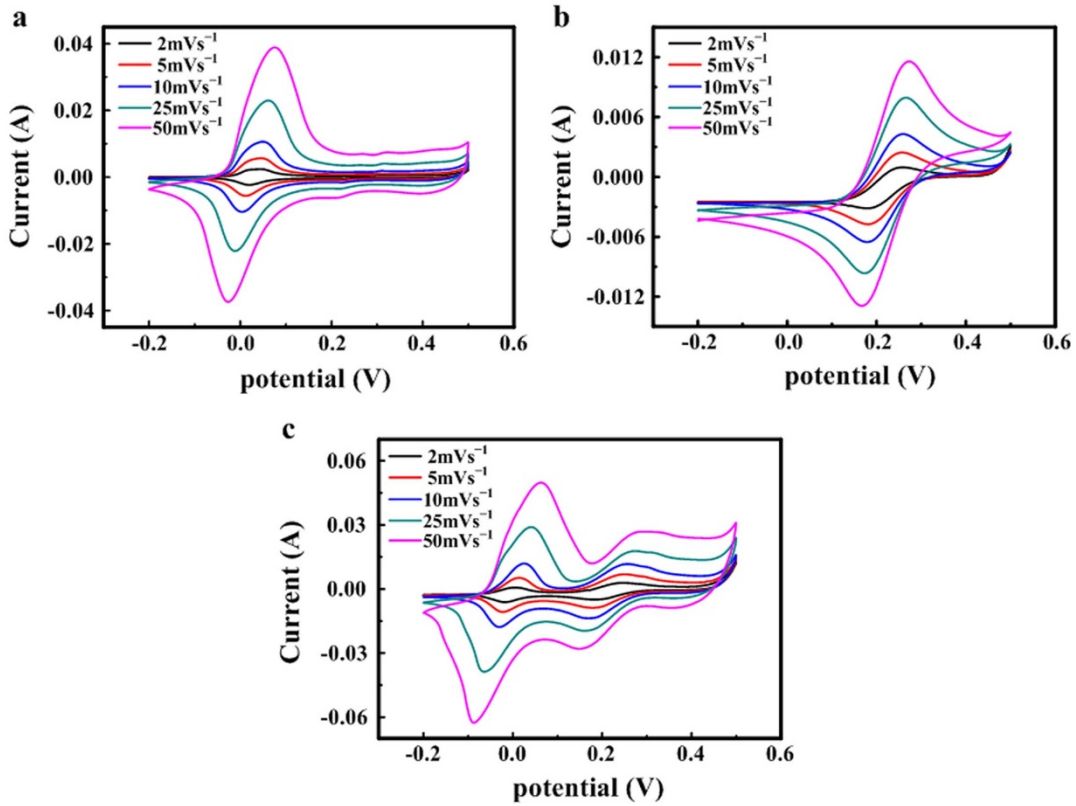

Figure 1 | **Cyclic voltammograms at different scan rates (2, 5, 10, 25 and 50 mVs^{-1}) for system: Co(OH)$_2$/GNS electrode in 1 M KOH solution (a), platinum electrode in mixed 1 M KOH and 0.04 M K$_3$Fe(CN)$_6$ solution (b), and Co(OH)$_2$/GNS electrode in mixed 1 M KOH and 0.04 M K$_3$Fe(CN)$_6$ solution (c).**

0.18 V in discharging process, corresponding to the redox reaction of $K_3Fe(CN)_6$. The potential plateaus result from a lot of exchanges occurred between electrons, corresponding to the anodic and cathodic peaks in the CV curves. The specific capacitance and coulombic efficiency for the two systems can be determined based on the equation (3) and (4), respectively. From the galvanostatic charge-discharge curve at 16 Ag^{-1} (32 Ag^{-1}), the specific capacitance for system 1 is 567.3 Fg^{-1} (517.8 Fg^{-1}), while that for system 3 is 2434.9 Fg^{-1} (1733.0 Fg^{-1}). The coulombic efficiency for system 1 is 93.2% (90.6%), and 163.8% (121.6%) for system 3. The high specific capacitance for system 3 is due to that both $Co(OH)_2$ and $K_3Fe(CN)_6$ directly do contribute the pseudocapacitance to the system 3, while only $Co(OH)_2$ gives a contribution of pseudocapacitance to system 1. As for the high coulombic efficiency for system 3, it can be explained by that for the initial additive of $Fe(CN)_6^{3-}$, according to the equation (2), in discharging process, only part of $Fe(CN)_6^{3-}$ gains an electron and is reduced into $Fe(CN)_6^{4-}$, while in charging process, $Fe(CN)_6^{4-}$ loses an electron and is completely oxidized into $Fe(CN)_6^{3-}$. Since the released charges include both discharging and no discharging $Fe(CN)_6^{3-}$, which can be much more than reserved charges in charging process. This is the reason why the coulombic efficiency is larger than 100%. For example, the electric charge with a quantity of 77.2 C for system 3 can be completely released from 0.04 M $K_3Fe(CN)_6$ in 20 mL solution, if all $K_3Fe(CN)_6$ is reduced into $K_4Fe(CN)_6$. In fact, in a single charge-discharge process for $K_3Fe(CN)_6$ electrolyte, the electric charge with a quantity of 0.024 C is charged accompanied by the change of $K_4Fe(CN)_6$ into $K_3Fe(CN)_6$, and 0.027 C is discharged accompanied

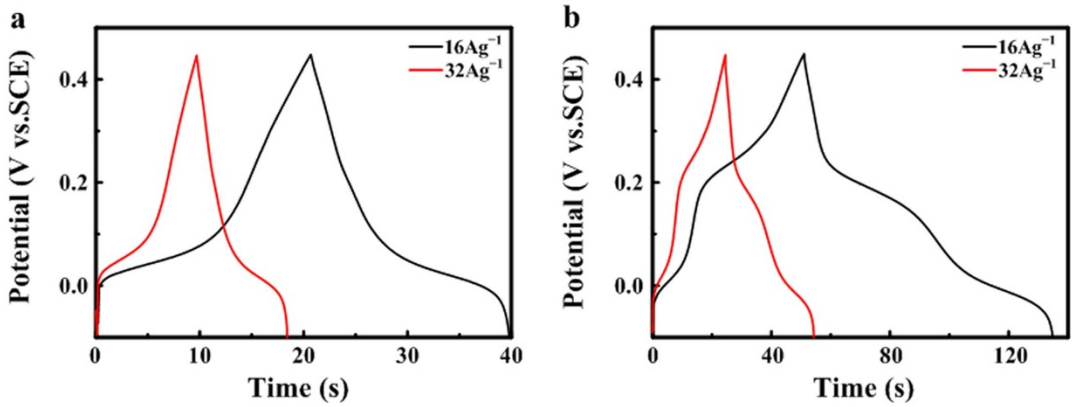

Figure 2 | **Galvanostatic charge-discharge curves at different current densities for Co(OH)$_2$/GNS electrode in 1 M KOH solution (a) and Co(OH)$_2$/GNS electrode in mixed 1 M KOH and 0.04 M K$_3$Fe(CN)$_6$ solution (b).**

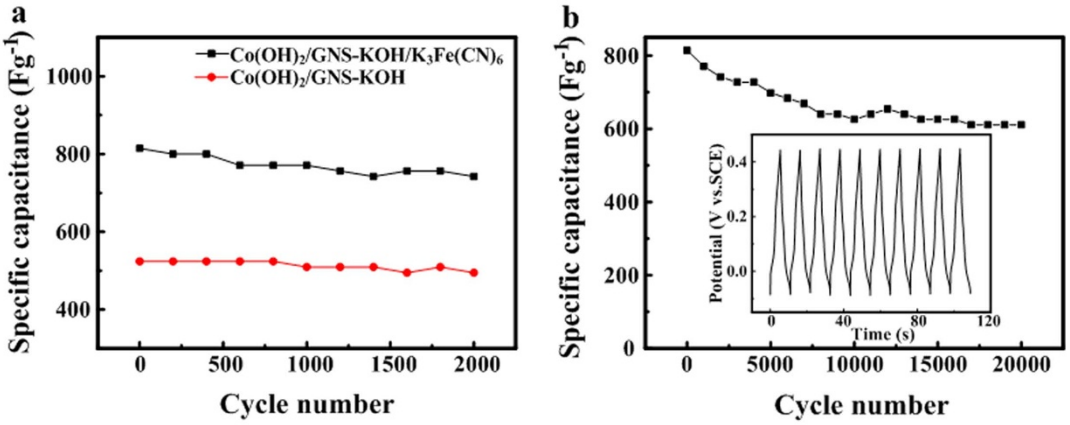

Figure 3 | Cycling performance of $Co(OH)_2$/GNS electrode in 1 M KOH and $Co(OH)_2$/GNS electrode in mixed 1 M KOH and 0.04 M $K_3Fe(CN)_6$ solution for 2000 cycles (a) and $Co(OH)_2$/GNS electrode in mixed 1 M KOH and 0.04 M $K_3Fe(CN)_6$ solution for 20000 cycles (b), measured by using the galvanostatic charge-discharge technique at a current density of 80 Ag^{-1}.

by the change of $K_3Fe(CN)_6$ into $K_4Fe(CN)_6$ for system 2 (both positive and negative electrodes consist of platinum plate). After each cycling, the $K_3Fe(CN)_6$ concentration in KOH electrolyte changes slightly (only 0.04‰ of $K_3Fe(CN)_6$ after each cycling is consumed) compared with that at the initial state, demonstrating that KOH/$K_3Fe(CN)_6$ electrolyte is similar to a constant buffer solution. Hence the high coulombic efficiency (more than 100%) can be maintained for a long time. In particular, if the pseudocapacitance mainly comes from $Co(OH)_2$, rather than $K_3Fe(CN)_6$, the $K_3Fe(CN)_6$ will be consumed slowly, resulting in a long electrochemical stability for system 3. However, the coulombic efficiency decreases with increasing cycle number, which can be attributed to the consumption of $Fe(CN)_6^{3-}$ in each discharging process. The high coulombic efficiency is essential for a battery-type supercapacitor device with a high energy density. In the practical application, the high coulombic efficiency can be recovered via only charging the electrolyte containing $K_4Fe(CN)_6$. As the electrolyte is applied at a high constant potential, $Fe(CN)_6^{4-}$ will be oxidized completely. As a result, all $K_4Fe(CN)_6$ can be transformed into $K_3Fe(CN)_6$, and the high coulombic efficiency can be recovered (Supporting materials 3).

The electrochemical stability is a very important factor for determining the capacitive properties of pseudocapacitors with introduction of additive into electrolyte. The cycling stability for either system 1 or 3 is examined by continuous charge-discharge experiments for 2000 cycles at a high current density of 80 Ag^{-1}, as shown in Fig. 3(a). Both systems exhibit a high cycling stability, with retention of 94.4% and 91.1% initial capacitance after 2000 cycles. This indicates that either system 1 or 3 is stable and the addition of $K_3Fe(CN)_6$ into KOH electrolyte does not obviously affect the stability of the electrode material, which is consistent with the results from XRD and SEM. The cycling stability of system 3 is also performed at 80 Ag^{-1} for 20000 continuous charge-discharge cycles, as shown in Fig. 3(b), from which the system maintains a high specific capacitance of 610.9 Fg^{-1} after 20000 cycles, and retention of 75.0% the initial specific capacitance (814.5 Fg^{-1}), indicating that the novel $Co(OH)_2$/GNS-KOH/$K_3Fe(CN)_6$ system exhibits a high electrochemical activity and excellent cycling stability.

The comparison in electrical conductivity between system 1 and 3, determined by the electrochemical impedance spectroscopy (EIS) measurements, is shown in Fig. 4, from which system 3 possesses a smaller interfacial charge-transfer resistance (R_{ct}, calculated from the span of the single semi-circle along the x-axis from the high to low frequency region) and lower internal resistance (R_i, the intersecting point with the x-axis in the range of high frequency), compared to system 1. Such a pattern of the plots can be fitted by that from an equivalent circuit in the inset of Fig. 4, in which R_{ct} = 0.1 $m\Omega$ and R_i = 300.9 $m\Omega$ for system 3, while R_{ct} = 10.0 $m\Omega$ and R_i = 500.2 $m\Omega$ for system 1[26,27]. The lower resistance for system 3 can afford a facile ionic and electronic transfer to ensure a high capacitive performance. Clearly, the electrochemical performances for system 3 are enhanced remarkably after introducing the redox mediator of $K_3Fe(CN)_6$ into KOH electrolyte.

Finally, the effect of the $K_3Fe(CN)_6$ concentration in KOH electrolyte on the pesudocapacitive properties for system 3 is explored, and the CV curves for system 3 with a concentration $K_3Fe(CN)_6$ of 0.00, 0.01, 0.02, 0.04, 0.06 and 0.08 M, respectively, at a scan rate of 25 mVs^{-1}, are shown in Fig. 5(a). The peak current from $Co(OH)_2$ decreases slightly first, then increases, and finally almost keeps constant, and that from $K_3Fe(CN)_6$ increases obviously with increasing the $K_3Fe(CN)_6$ concentration (Supporting materials 4), indicating the capacitance contributed by $Co(OH)_2$ decreases slightly first, then increases, and finally almost keeps constant. In contrast, the capacitance contributed by $K_3Fe(CN)_6$ increases obviously. The peak currents for the oxidation of $Co(OH)_2$ and reduction of CoOOH are depressed, resulting from the adsorption of $Fe(CN)_6^{3-}$/$Fe(CN)_6^{4-}$ on the $Co(OH)_2$/GNS electrode surface, which suppresses the OH^- diffusion. This suppression leads to a shortage of OH^-, decreasing the reaction rate of $Co(OH)_2$/CoOOH. On the other hand, upon further increasing the $K_3Fe(CN)_6$ concentration, more $Fe(CN)_6^{3-}$/$Fe(CN)_6^{4-}$ ions play the role of "electron shuttle" in the charge/discharge processes of $Co(OH)_2$/CoOOH, promoting a high activity of $Co(OH)_2$/CoOOH[24]. This promotion results in an increase

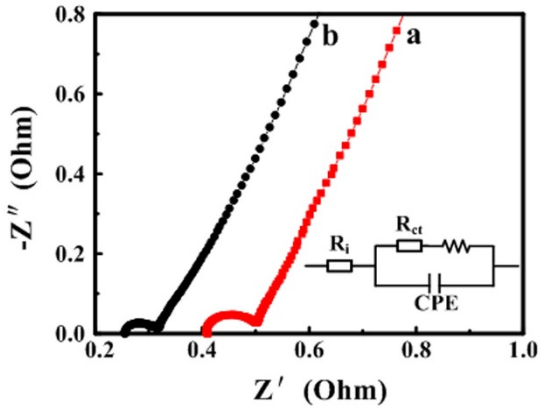

Figure 4 | Nyquist plots of $Co(OH)_2$/GNS electrode in 1 M KOH (a) and $Co(OH)_2$/GNS electrode in mixed 1 M KOH and 0.04 M $K_3Fe(CN)_6$ solution (b), in which the inset shows the equivalent circuit.

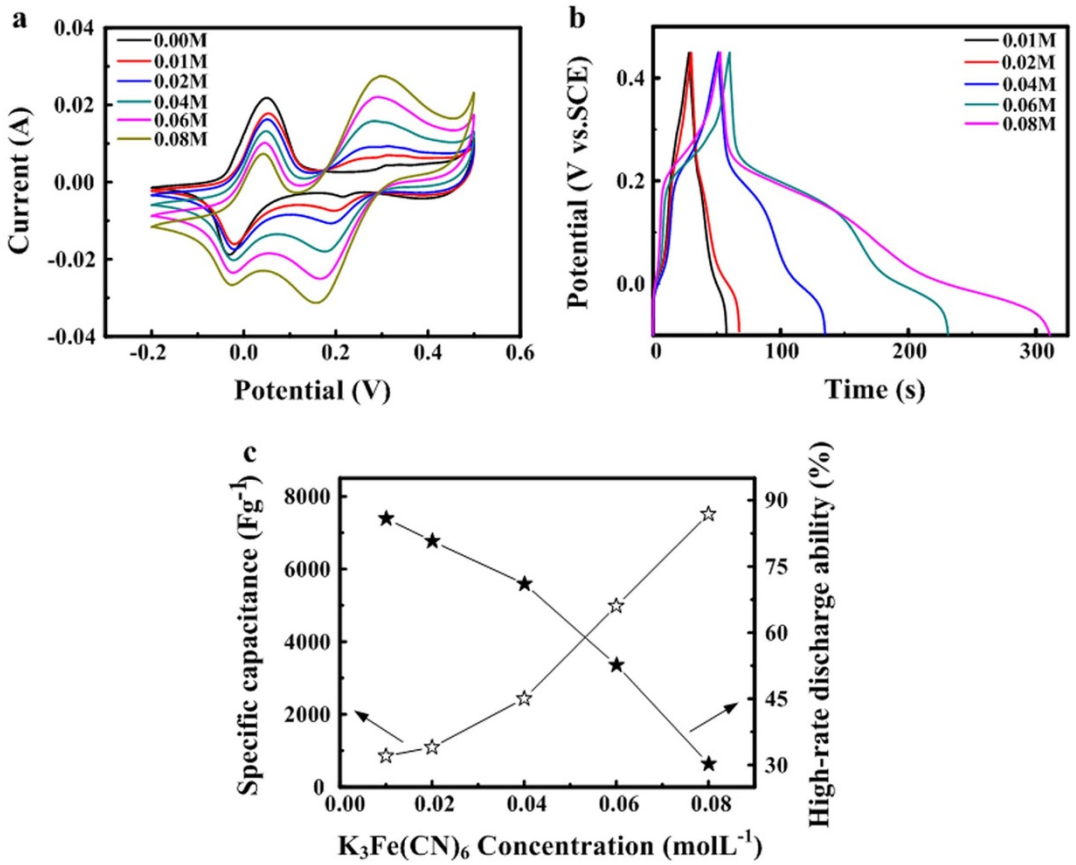

Figure 5 | Cyclic voltammograms at a scan rate of 25 mVs^{-1} (a), Galvanostatic charge-discharge curves at a current density of 16 Ag^{-1} (b), specific capacitance and high-rate discharge ability vs. different $K_3Fe(CN)_6$ concentrations (c) for the system of $Co(OH)_2$/GNS electrode in 1 M KOH containing different concentrations of $K_3Fe(CN)_6$ mixed solution.

in peak current. As above two effects are balanced, the peak current keeps almost constant. In addition, anodic and cathodic peak currents corresponding to redox reaction of $Co(OH)_2$/CoOOH downshift, which is also caused by electrostatic adsorption, the more $Fe(CN)_6^{3-}/Fe(CN)_6^{4-}$ ions are adsorbed on the $Co(OH)_2$ electrode surface, the larger the resistance to OH^- diffusion is. In Fig. 5(b), as the $K_3Fe(CN)_6$ concentration in system 3 is 0.01, 0.02, 0.04, 0.06 and 0.08 M, respectively, the specific capacitance, evaluated at a high current density of 16 Ag^{-1} from charge-discharge curves, will be 852.4, 1093.8, 2434.9, 4983.3 and 7514.2 Fg^{-1}, respectively, corresponding to the coulombic efficiency of 103.9%, 125.8%, 163.8%, 285.5% and 541.4%, respectively (charge and discharge time are listed in Table 1). The system can be charged quickly, and discharged slowly, which means that the promise can be offered to realize a battery-type supercapacitor. In addition, if the high-rate discharge ability (HRD) of the electrode is defined as the ratio of discharge capacitance at 32 Ag^{-1} to that at 16 Ag^{-1}, the HRD for system 3 containing $K_3Fe(CN)_6$ with a concentration of 0.01, 0.02, 0.04, 0.06 and 0.08 M, respectively, will be 86.0%, 80.9%, 71.2%, 52.8% and 30.4%, respectively. The typical data about the specific capacitance and HRD for system 3 containing various of $K_3Fe(CN)_6$ concentrations are shown in Fig. 5(c). When the $K_3Fe(CN)_6$ concentration is lower, the contribution of the redox reaction from $K_3Fe(CN)_6$ is lower, resulting in a low specific capacitance. However, high concentration and charge-discharge current density will cause high concentration polarization, leading to a low rate property and poor electrochemical stability. From above, the $K_3Fe(CN)_6$ concentration has a significant influence on the specific capacitance, coulombic efficiency and rate property. High $K_3Fe(CN)_6$ concentration facilitates a high specific capacitance and coulombic efficiency, but worsens a rate property and electrochemical stability. Therefore, only the $K_3Fe(CN)_6$ concentration is proper, the energy density, power density, coulombic efficiency, and long-term cycle life can be compromised. For one system, a high specific capacitance indicates a high energy density, while a high power density associates with a large current charge-discharge characteristic. Through well controlling the $K_3Fe(CN)_6$ concentration, a novel system with high energy density, power density, coulombic efficiency and long-term cycle life can be realized.

Discussion

In summary, a simple and effective method has been implemented to enhance the electrochemical performance for $Co(OH)_2$/GNS electrode through introducing $K_3Fe(CN)_6$ into the conventional KOH electrolyte. As both solid electrode and liquid electrolyte can contribute to the pseudocapacitance simultaneously, an ultrahigh capacitive performance has been realized. The system exhibits not only an

Table 1 | Charge and discharge time for $Co(OH)_2$/GNS electrode in 1 M KOH containing different concentrations of $K_3Fe(CN)_6$ mixed solution, calculated from galvanostatic charge-discharge curves at a current density of 16 Ag^{-1}

Concentration (M)	*Charge time (s)*	*Discharge time (s)*
0.01	28.2	29.3
0.02	29.9	37.6
0.04	51.1	83.7
0.06	60.0	171.3
0.08	52.7	285.3

ultrahigh specific capacitance and coulombic efficiency (a maximum specific capacitance of 7514.2 Fg^{-1} and coulombic efficiency of 541.4% at a high current density of 16 Ag^{-1} in the mixed 1 M KOH and 0.08 M $K_3Fe(CN)_6$ solution), but also an excellent cycling stability (the capacitance retention is 91.1% after 2000 continuous charge-discharge cycles and 75.0% after 20000 continuous cycles at 80 Ag^{-1} in mixed 1 M KOH and 0.04 M $K_3Fe(CN)_6$ solution). Upon increasing the $K_3Fe(CN)_6$ concentration, both specific capacitance and coulombic efficiency increase, but the rate property is worsened. The energy density and power density for the system can be compromised via well controlling the $K_3Fe(CN)_6$ concentration according to the practical application, and the high coulombic efficiency (more than 100%) can be recovered by charging the electrolyte. This encouraging investigation shows great potential in developing a battery-type supercapacitor with a high energy density, power density, coulombic efficiency and long-term cycling stability.

Methods

Vertically oriented GNS were synthesized by radio-frequency plasma-enhanced chemical vapour deposition (RF-PECVD) on nickel-foam used as substrates for cathodic electrodeposition of $Co(OH)_2$ nanosheets in $Co(NO_3)_2$ aqueous solution, the detailed description about the preparation can be found in ref. [25]. The microstructure and surface morphology of the electrode materials were characterized by X-ray diffraction (XRD) (RIGAKU D/MAX2500), and field emission scanning electron microscopy (FE-SEM) (JEOL JSM-6700F). Electrochemical measurements were carried out via a computer-controlled electrochemical working station (CHI760D or PARSTAT2273) with a conventional three-electrode electrochemical cell. The electrolytes were 1 M KOH aqueous solution with or without $K_3Fe(CN)_6$ with different concentrations. The working electrode was the prepared $Co(OH)_2$/GNS/Ni foam, and a platinum plate and a saturated calomel electrode (SCE) were used as counter electrode and reference electrode, respectively. The specific capacitance of the system is calculated from galvanostatic charge-discharge curves according to equation (3):

$$Cm = \frac{I \times \Delta t}{\Delta V \times m} \tag{3}$$

where I (A) is discharging current, Δt (s) is discharging time, ΔV (V) is potential drop during discharging process, and m (g) is mass of the $Co(OH)_2$. Another important parameter coulombic efficiency (η) is evaluated from equation (4):

$$\eta = \frac{t_D}{t_C} \times 100\% \tag{4}$$

where t_D and t_C are discharging time and charging time, respectively.

1. Conway, B. E. Electrochemical Supercapacitors: Scientific Fundamentals and Technological Applications (Kluwer-Academic, 1999).
2. Seung, W. L., Betar, M. G., Hye, R. B., Paula, T. H. & Yang, S. H. Nanostructured carbon-based electrodes: bridging the gap between thin-film lithium-ion batteries and electrochemical capacitors. *Energy Environ. Sci.* **4**, 1972–1985 (2011).
3. Zhai, Y. P. *et al.* Carbon Materials for Chemical Capacitive Energy Storage. *Adv. Mater.* **23**, 4828–4850 (2011).
4. Simon, P. & Gogotsi, Y. Materials for electrochemical capacitors. *Nat. Mater.* **7**, 845–854 (2008).
5. Zhang, L. L. & Zhao, X. S. Graphene-based nanomaterials for energy storage. *Chem. Soc. Rev.* **38**, 2520–2531 (2009).
6. Zhang, H. G., Yu, X. D. & Braun, P. V. Three-dimensional bicontinuous ultrafast-charge and -discharge bulk battery electrodes. *Nature Nanotech.* **6**, 277–281 (2011).
7. Kang, B. & Ceder, G. Battery materials for ultrafast charging and discharging. *Nature* **458**, 190–193 (2009).
8. Lee, S. W. *et al.* High-power lithium batteries from functionalized carbon-nanotube electrodes. *Nat. Nanotechnol.* **5**, 531–537 (2010).
9. Liu, C. G., Yu, Z. N., Neff, D., Zhamu, A. & Jang, B. Z. Graphene-Based Supercapacitor with an Ultrahigh Energy Density. *Nano Lett.* **10**, 4863–4868 (2010).
10. Centeno, T. A., Hahn, M., Fernandez, J. A., Kotz, R. & Stoeckli, F. Correlation between capacitances of porous carbons in acidic and aprotic EDLC electrolytes. *Electrochem. Commun.* **9**, 1242–1246 (2007).
11. Fan, Z. J. *et al.* Asymmetric Supercapacitors Based on Graphene/MnO_2 and Activated Carbon Nanofiber Electrodes with High Power and Energy Density. *Adv. Funct. Mater.* **21**, 2366–2375 (2011).
12. Wang, G. P., Zhang, L. & Zhang, J. J. A review of electrode materials for electrochemical supercapacitors. *Chem. Soc. Rev.* **41**, 797–828 (2012).
13. Largeot, C. *et al.* Relation between the Ion Size and Pore Size for an Electric Double-Layer Capacitor. *J. Am. Chem. Soc.* **130**, 2730–2731 (2008).
14. Wang, H. L., Casalongue, H. S., Liang, Y. Y. & Dai, H. J. $Ni(OH)_2$ nanoplates grown on graphene as advanced electrochemical pseudocapacitor materials. *J. Am. Chem. Soc.* **132**, 7472–7477 (2010).
15. Augustyn, V. *et al.* High-rate electrochemical energy storage through Li^+ intercalation pseudocapacitance. *Nat. Mater.* **12**, 518–522 (2013).
16. Lang, X. Y., Hirata, A., Fujita, T. & Chen, M. W. Nanoporous metal/oxide hybrid electrodes for electrochemical supercapacitors. *Nature Nanotech.* **6**, 232–236 (2011).
17. Yang, L. *et al.* Hierarchical network architectures of carbon fiber paper supported Cobalt Oxide nanonet for high-capacity pseudocapacitors. *Nano Lett.* **12**, 321–325 (2012).
18. Xia, X. H. *et al.* Graphene sheet/porous NiO hybrid film for supercapacitor applications. *Chem. Eur. J.* **17**, 10898–10905 (2011).
19. Arico, A. S., Bruce, P., Scrosati, B., Tarascon, J. M. & Van Schalkwijk, W. Nanostructured materials for advanced energy conversion and storage devices. *Nat. Mater.* **4**, 366–377 (2005).
20. Wu, J. H. *et al.* A simple and high-effective electrolyte mediated with p-phenylenediamine for supercapacitor. *J. Mater. Chem.* **22**, 19025–19030 (2012).
21. Roldan, S., Granda, M., Menendez, R., Santamaría, R. & Blanco, C. Mechanisms of Energy Storage in Carbon-Based Supercapacitors Modified with a Quinoid Redox-Active Electrolyte. *J. Phys. Chem. C* **115**, 17606–17611 (2011).
22. Chen, W., Rakhi, R. B. & Alshareef, H. N. Capacitance enhancement of polyaniline coated curved-graphene supercapacitors in a redox-active electrolyte. *Nanoscale* **5**, 4134–4138 (2013).
23. Senthilkumar, S. T., Selvan, R. K., Lee, Y. S. & Melo, J. S. Electric double layer capacitor and its improved specific capacitance using redox additive electrolyte. *J. Mater. Chem. A* **1**, 1086–1095 (2013).
24. Su, L. H., Zhang, X. G., Mi, C. H., Gao, B. & Liu, Y. Improvement of the capacitive performances for Co-Al layered double hydroxide by adding hexacyanoferrate into the electrolyte. *Phys. Chem. Chem. Phys.* **11**, 2195–2202 (2009).
25. Zhao, C. M. *et al.* Synthesis of $Co(OH)_2$/graphene/Ni foam nano-electrodes with excellent pseudocapacitive behavior and high cycling stability for Supercapacitors. *Int. J. Hydrogen Energy* **37**, 11846–11852 (2012).
26. Wang, H., Ma, D., Huang, X., Huang, Y. & Zhang, X. General and Controllable Synthesis Strategy of Metal Oxide/TiO_2 Hierarchical Heterostructures with Improved Lithium-Ion Battery Performance. *Sci. Rep.* **2**, 701–708 (2012).
27. Zhang, L. *et al.* Porous 3D graphene-based bulk materials with exceptional high surface area and excellent conductivity for supercapacitors. *Sci. Rep.* **3**, 1408–1416 (2013).

Acknowledgments

The support from National Natural Science Foundation of China (Grant Nos. 50525204 and 50832001), the special Ph.D. program (Grant No. 200801830025) from MOE, Major science and technology project of Jilin Province (Grant No. 11ZDGG010), NSF of China (grant no. 51372095), program for Changjiang Scholars and Innovative Research Team in University, the "211" and "985" project of Jilin University, China, is highly appreciated.

Author contributions

W.Z. and C.Z. planned and performed the experiments, collected and analysed the data, and wrote the paper. X.W., H.Z. and X.C. involved in analysing the results and writing the paper. H.W. helped to synthesize and characterize the samples. All authors discussed the results and commented on the manuscript.

Additional information

Supplementary information accompanies this paper at http://www.nature.com/scientificreports

Competing financial interests: The authors declare no competing financial interests.

How to cite this article: Zhao, C.M. *et al.* Ultrahigh capacitive performance from both $Co(OH)_2$/graphene electrode and $K_3Fe(CN)_6$ electrolyte. *Sci. Rep.* **3**, 2986; DOI:10.1038/srep02986 (2013).